Biosensors and Bioelectronics 51 (2014) 362–365

Contents lists available at ScienceDirect

Biosensors and Bioelectronics

journal homepage: www.elsevier.com/locate/bios

Short communication

Low-temperature fabrication of ZnO nanorods/ferrocenyl–alkanethiol bilayer electrode and its application for enzymatic glucose detection

Qiang Ma [a,b,*], Kazuo Nakazato [a,b]

[a] Department of Electrical Engineering and Computer Science, Nagoya University, Nagoya 464-8603, Japan
[b] Venture Business Laboratory, Nagoya University, Nagoya 464-8603, Japan

ARTICLE INFO

Article history:
Received 14 May 2013
Received in revised form
20 July 2013
Accepted 5 August 2013
Available online 22 August 2013

Keywords:
Zinc oxide
Nanorods
Enzymatic glucose sensor
Ferrocenyl–alkanethiol

ABSTRACT

A novel ZnO nanorods/ferrocenyl–alkanethiol ($FcC_{11}SH$) bilayer structure was prepared and applied for the fabrication of glucose enzymatic biosensor. ZnO nanorod matrix was synthesized by low temperature aqueous method and provided a favorable environment for the immobilization of glucose oxidase (GOx). A monolayer of $FcC_{11}SH$ molecular was self-assembled on the surface of gold electrode and introduced a shuttling way for electronic communication between GOx and electrode. The morphology and structure of prepared ZnO nanorods were characterized by employing scanning electron microscopy (SEM), and X-ray powder diffraction (XRD). Electrochemcial measurements of the sensor revealed a high and reproducible sensitivity of 27.8 $\mu A\ cm^{-2}\ mM^{-1}$, and a linear range from 0.05 to 1.0 mM with a detection limit of 20 μM. A relatively low value of Michaelis–Menten constant about 2.95 mM indicates the enhanced affinity of GOx to glucose. To the best of our knowledge, this is the first time to fabricate the glucose biosensor by using ZnO and $FcC_{11}SH$ bilayer structure.

1. Introduction

As an important II–VI group semiconductor, zinc oxide (ZnO) has numerous potential applications in solar cells, transistors, gas sensors and actuators (Huang et al., 2001; Kim and Fujita, 2002; Ahmad et al., 2013). Especially, one-dimensional ZnO nanostructures show great promise on electrochemical application due to their unique properties including nontoxicity, chemical stability, vast surface-to-bulk ratio, and fast electron communication features (Wei et al., 2010; Umar et al., 2007). Since Clark and Lyons proposed the first glucose enzyme electrode in 1962 (Clark and Lyons, 1962), various materials and complex layers have been investigated intensively and applied for glucose measurement (Umar et al., 2009a, 2009b; Meredith and Minteer, 2011; Fang et al., 2011; Qiu et al., 2007; Li and Zhou, 2013; Zhao et al., 2013a; Wang et al., 2008; Chen et al., 2013; Forzani et al., 2004; Rahman et al., 2009a; Lee et al., 2007; Liu et al., 2011, 2012; Ding et al., 2012; Huang et al., 2013). Because for a high isoelectric point (IEP) of about 9.5, ZnO nanostructure matrix can provide a positively charged substrate for immobilizing low IEP glucose oxidase (=4.2) at physiological pH of 7.4. To date, different kinds of ZnO nanostructures have been used to fabricate different kind of enzymatic biosensors (Zhao et al., 2007, 2013b; Liu et al., 2009; Ahmad et al., 2010; Zang et al., 2007). However, the absence of redox centers in ZnO is causing a hindrance toward the performance of glucose sensor. It is crucial to introduce certain extrinsic redox species into ZnO-based biosensors to provide a shuttling path for electrons transfer from the enzyme to the electrode. As well known, 11-ferrocenyl-1-undecanethiol ($FcC_{11}SH$) has been proved to be useful as redox mediators to enhance the rate of electronic communication (Ju and Leech, 1999; Creager and Rowe, 1994; Patela et al., 2003). The ferrocene group located at the end of the alkyl chain plays a crucial role on generating a large redox current. Some groups have employed ferrocene-terminated alkanethiols to fabricate good performance biosensor (Ghica and Brett, 2005; Peng et al., 2011). However, basing on our knowledge, only few reports ever mentioned its application on glucose biosensor.

In this letter, we developed a novel glucose sensor based on ZnO nanorods and $FcC_{11}SH$ bilayer modified gold electrodes. At first, a layer of $FcC_{11}SH$ molecular was assembled on Au electrode and acted as redox mediator to improve the electronic communication. Then, ZnO nanorods arrays were synthesized directly on the self-assembled monolayer of $FcC_{11}SH$ by low temperature aqueous method under atmospheric pressure. In contrast to other growth methods, due to the low growth temperature, $FcC_{11}SH$ molecular can be protected from thermal damage. Electrochemical workstation was used to study the basic self-assembling and electrochemical features of biosensor.

* Corresponding author at: Department of Electrical Engineering and Computer Science, Nagoya University, Nagoya 464-8603, Japan. Tel.: +81 52 736 7577.
E-mail address: maqiang0710@gmail.com (Q. Ma).

0956-5663/$ - see front matter © 2013 Elsevier B.V. All rights reserved.
http://dx.doi.org/10.1016/j.bios.2013.08.004

2. Materials and methods

2.1. Self-assembling of $FcC_{11}SH$

Silicon (100) wafers, covered with 20 nm Ti film and 100 nm Au film, were employed as the electrodes of glucose sensor. The electrodes were immersed in a 5 mM ethanol solution of $FcC_{11}SH$ for 16 h. After self-assembling, the electrodes were rinsed with ethanol and deionized water twice to remove unreacted biomolecules. Then, they were kept in a 0.1 M sodium sulfate solution at 4 °C until use.

2.2. Synthesis of ZnO nanorods

ZnO nanorods arrays were grown directly on the $FcC_{11}SH$-assembled electrodes by two-step chemical solution method. Firstly, a seed layer of ZnO nanocrystal was prepared by cathodic electrochemical deposition from an aqueous solution of zinc nitrate ($Zn(NO_3)_2$, 10 mM) at room temperature. A metal Pt wire and the electrodes were used as anode and cathode, respectively. Secondly, the growth of ZnO nanorods was realized by using chemical bath deposition. Precursor solutions of 10 mM $Zn(NO_3)_2$ and 10 mM hexamethylenetetramine ($C_6H_{12}N_4$) were mixed under continuous stirring in glass flask. The electrodes with seed layer were immersed into the precursor solution vertically. The flask was placed in 80 °C water bath for 6 h, and then cooled to room temperature.

2.3. Fabrication of Naf/GOx/ZnO/$FcC_{11}SH$/Au electrode

For immobilization of GOx, a 20 uL GOx (10 mg/ml in 0.01 M phosphate buffer saline, PBS) solution was dropped onto the surface of the ZnO/$FcC_{11}SH$/Au electrode. The electrodes were kept overnight for enzyme immobilization. Subsequently, the electrodes were rinsed with PBS to remove the loosely adsorbed GOx. Finally, 10 μl 1.0% Nafion solution was used to attach GOx/ZnO nanorods tightly on the surface of electrodes.

2.4. Characterizations of Naf/GOx/ZnO/$FcC_{11}SH$/Au electrode

The morphology and structure of prepared ZnO nanorods were characterized by scanning electron microscopy (SEM), and X-ray powder diffraction (XRD). Electrochemical measurements were carried out with an Electrochemical Workstation in a conventional three-electrode system. All the measurement temperatures were kept at room temperature.

3. Results and discussion

Fig. 1 shows SEM images for the ZnO nanorods grown on $FcC_{11}SH$ modified Au electrodes. ZnO nanorods cover the entire surface of electrodes with high density. Fig. 1(b) and (c) show cross-sectional view and enlarged top view of ZnO nanorod arrays, respectively. After 6 h of growth, ZnO nanorods exhibit hexagonal rod shape, with about 100–300 nm in diameter, and several micrometers in length. The crystalline structure of ZnO nanorods was investigated by XRD measurements. A representative pattern of the as-prepared ZnO products is shown in Fig. 1(d), the diffraction spectrum shows a (002) peak with relatively strong intensities. It is also detected other diffraction peaks with a much lower intensity mainly at 31.7° and 36.2°, 47.5°, 56.6°and 62.8° corresponding to the following lattice planes: (100), (101), (102), (110), and (103) (Saha et al., 2010). The diffraction spectrum indicates that the crystalline structure of ZnO nanorods is wurtzite structure.

To check the chemical stability and sensitivity of $FcC_{11}SH$ molecules, Fig. 2 shows cyclic voltammetric sweep curves for the $FcC_{11}SH$/Au electrode (Fig. 2(a)) and the ZnO/$FcC_{11}SH$/Au electrode (Fig. 2(b)) in 0.2 M solution of sodium perchlorate ($NaClO_4$). A pair

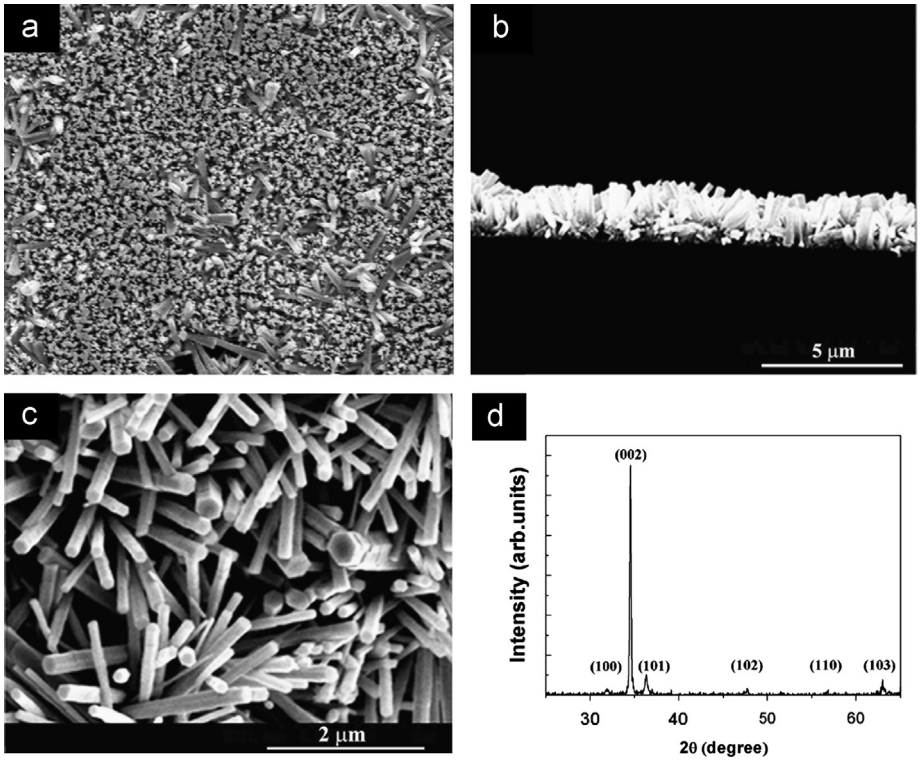

Fig. 1. SEM image of ZnO nanorod arrays on SAM of $FcC_{11}SH$ modified Au electrode: (a) top view, (b) side view, (c) high magnification; and (d) XRD spectra of low-temperature grown ZnO nanorod arrays.

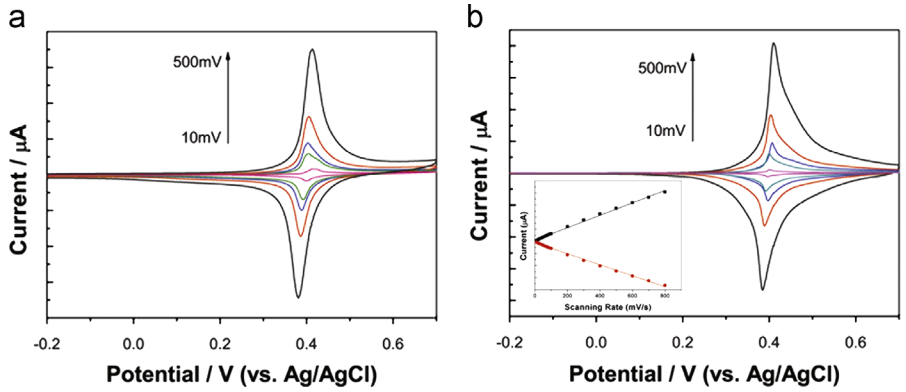

Fig. 2. Cyclic voltammetric sweep curves for (a) FcC11SH/Au electrode and (b) ZnO/FcC_{11}SH/Au electrode in 0.2 M solution of $NaClO_4$ at various scan rates from 0.01 V/s to 0.5 V/s.

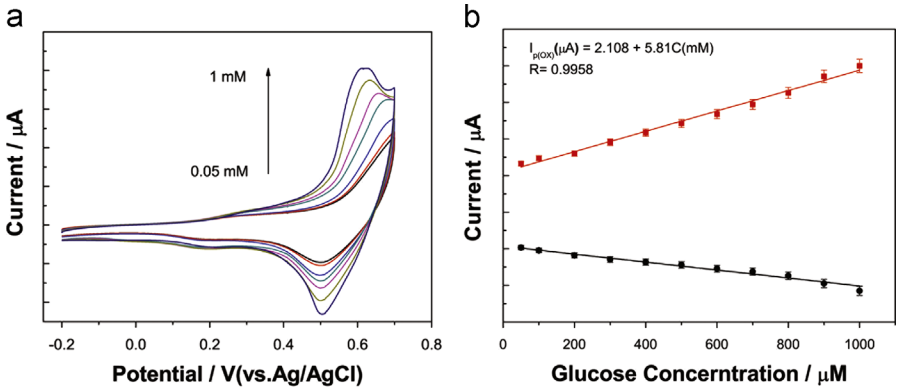

Fig. 3. (a) Cyclic voltammetric characteristics of Naf/GOx/ZnO/FcC_{11}SH/Au electrode with successive increments of glucose concentrations from 50 μM to 1 mM; (b) The calibration curve of the response current of sensors to glucose solutions of different concentrations. A potential of +0.6 V (vs. Ag/AgCl reference) was applied on the working electrode in the measurement. Error bars represented standard deviations (RSD=4.8%, n=3).

of oxidation–reduction peaks of ferrocenium/ferrocene (Fc^+/Fc°) couple, with potential of 0.406 V and 0.398 V, was detected in both Fig. 2(a) and (b), respectively. The emergence of these peaks can be attributed to the effect of reaction between ferrocene (Fc) and acid counteranions (ClO_4^-) (Rahman et al., 2009b). Moreover, the redox peak currents linearly increased simultaneously with the scan rate for values from 0.01 to 0.5 V/s, $Ip_{(OX)}=3.247+0.731v$ (R=0.9986) and $Ip_{(R)}=-3.210-0.638v$ (R=0.9983). Meanwhile, the peak-to-peak separation also increased. These results reveal that the electron transfer between FcC_{11}SH and Au microelectrode can be easily performed and is a surface-controlled electrochemical process (Ju and Leech, 1999; Creager and Rowe, 1994; Patela et al., 2003; Ghica and Brett, 2005; Peng et al., 2011). Furthermore, the cyclic voltammetric curves in Fig. 2(b) also indicate that the electrochemical behavior of FcC_{11}SH molecular is kept well, even undergone the low temperature aqueous growth process of ZnO nanorod arrays.

The electrochemical performances of the FcC_{11}SH/Au electrode in PBS buffer were exhibited in Fig. S1. The redox peaks of Fc^+/Fc° couple (centered at ~0.52 V and ~0.48 V) were detected obviously. There were tiny changes on the central locations of the redox peak-to-peak. The linearity between the redox peak currents and the scan rate reveals that the electron transfer between FcC_{11}SH and Au microelectrode are stable and belongs to surface-controlled electrochemical process. We have investigated the *C–V* characteristics of Naf/GOx/FcC_{11}SH/Au electrode in pH 7.4 PBS buffer with different concentrations of glucose. The peak current of the electrode (~0.6 V) increased with successive increments of glucose concentrations. This result indicates that the monolayer of FcC_{11}SH molecular can introduce a shuttling way for electronic communication between GOx and electrode.

The main role of ZnO nanorods is to provide a favorable environment for the immobilization of GOx. We checked *C–V* curves for Naf/GOx/ZnO/Au and ZnO/Au in PBS buffer containing 1 mM glucose (Supporting information Fig. S2). The curve of GOx/ZnO/Au electrode showed an increase in current and a well-defined oxidation peak of glucose compared to ZnO/Au electrode. This phenomenon confirms the immobilization of GOx on the surface of nanorods. The peak currents of Naf/GOx/ZnO/Au electrode increased with the scan rate. This result illustrates a electrochemical behavior of surface diffusion process. Meantime, the adsorbed GOx on ZnO nanorods can keep its bioactivity under different scanning speed.

Fig. 3(a) shows the *C–V* characteristics of Naf/GOx/ZnO/FcC_{11}SH/Au electrode with successive increments of glucose concentrations in pH 7.4 PBS buffer with a sweep rate of 0.05 V/s. Higher glucose concentrations result in larger oxidation currents of bio-electrode. This phenomenon is attributed to the release of more number of electrons from the oxidized glucose and good catalytic behavior of FcC_{11}SH (Ghica and Brett, 2005; Peng et al., 2011). Moreover, the existence of FcC_{11}SH can provide an efficient conducting tunnel for electron transfer from the redox center of GOx to the electrode. The variation of current, measured at a fixed potential of 0.6 V for Naf/GOx/ZnO/FcC_{11}SH/Au electrode as a function of glucose concentration, is shown in Fig. 3(b). The linear response range of the sensor to glucose concentration is from 0.05 to 1 mM (correlation coefficient: 0.9958). The sensitivity of the composite bio-electrode is estimated to be 27.8 $\mu A\ mM^{-1}\ cm^{-2}$.

These data demonstrates that the device is in good linear relationship with glucose concentration. In addition, Michaelis–Menten constant (K_{Mapp}) is used to evaluate the enzymatic bioactivity for substrate, and calculated according to the Lineweaver–Burk equation (Salimi et al., 2010). The K_{Mapp} is calculated to be 2.95 mM, which is much lower than the value of free GOx (27 mM). The data indicates that the ZnO/FcC_{11}SH/Au electrode exhibits a higher affinity for glucose oxidase molecules. The sensitivity of the fabricated biosensor is relatively higher than those of previous reports and its K_{Mapp} is relatively lower (Zhao et al., 2007; Ahmad et al., 2013; Lei et al., 2010; Jung and Lim., 2012).

The electrocatalytic oxidation of glucose on Naf/GOx/ZnO/FcC_{11}SH/Au electrode can be described based on the following mechanism. At first, β-D-glucose will be catalyzed by GOx(OX) to produce D-glucono-δ-lactone, while GOx(OX) was changed into GOx(R). Meantime, the ferrocene moiety in FcC_{11}SH molecular is converted to ferricenium cation, which accepts an electron from the electrode. Then, the consumed GOx(OX) can be regenerated from GOx(R) through its reaction with the ferrocenium cation. The process of electrochemical glucose biosensors can be schematically illustrated according to the following reaction (Bourdillon et al., 1993; Salimi et al., 2010):

$$\beta\text{–D–glucose} + \mathrm{GOx(OX)} \rightarrow \text{D–glucono–}\delta\text{–lactone} + \mathrm{GOx}(R) \quad (1)$$

$$F_C \rightleftharpoons F_C^+ + e^- \quad (2)$$

$$2F_C^+ + \mathrm{GOx}(R) \rightarrow 2F_C + \mathrm{GOx(OX)} \quad (3)$$

where Fc is ferrocene, Fc^+ is a ferrocenium cation, GOx(OX) and GOx(R) represent oxidized and reduced forms of GOx respectively.

The selectivity testing of GOx/ZnO/FcC11SH electrode was done in 0.1 M PBS buffer (Supporting information, Fig. S3). The electrode gave out significant responses to incremental glucose concentrations. This indicates that the electrode shows a relatively good selectivity on the existence of glucose. In addition, when the electrodes were washed with PBS buffer and stored at 4 °C, the current response for the determination of glucose remained about 91% in 20 days, indicating that the performance of electrodes was stable.

4. Conclusions

In this work, we report an enzymatic glucose biosensor based on ZnO/FcC_{11}SH bilayer modified Au electrode. We employed a low temperature aqueous method to grow ZnO nanorod arrays on Au electrode with the SAM of FcC_{11}SH. On the one hand, this method realizes the low-cost fabrication of ZnO nanorod arrays, on the other hand protects the electrochemical properties of FcC_{11}SH from thermal damage. The electrochemical results of sensor show a high sensitivity of 27.8 μA μM^{-1} cm^{-2}, linear range from 50 μM to 1.0 mM. Basing on the research, low-cost glucose biosensor can be fabricated by using simple chemical/electrochemical method.

Acknowledgments

This work was supported by a Grant-in-Aid for Scientific Research (S) from the Ministry of Education, Culture, Sports, Science and Technology, Japan (20226009).

Appendix A. Supporting information

Supplementary data associated with this article can be found in the online version at http://dx.doi.org/10.1016/j.bios.2013.08.004.

References

Ahmad, R., Tripathy, N., Hahn, Y.B., 2013. Biosensors and Bioelectronics 45, 281–286.
Ahmad, M., Pan, C., Luo, Z., Zhu, J., 2010. Journal of Physical Chemistry C 114, 9308–9313.
Bourdillon, C., Demaille, C., Gueris, J., Morioux, J., Saveant, J.M., 1993. Journal of the American Chemical Society 115, 12264–12269.
Clark Jr., Lc., Lyons, C., 1962. Annals of the New York Academy of Sciences 102, 29–45.
Chen, L.J., Sun, B., Wang, X.D., Qiao, F.M., Ai, S.Y., 2013. Journal of Materials Chemistry B 1, 2268–2274.
Creager, S.E., Rowe, G.K., 1994. Journal of Electroanalytical Chemistry 420, 291–299.
Ding, R.M., Liu, J.P., Jiang, J., Zhu, J.H., Huang, X.T., 2012. Analytical Methods 4, 4003–4008.
Fang, B., Gu, A.X., Wang, G.F., Wang, W., Feng, Y.H., Zhang, C.H., Zhang, X.J., 2011. ACS Applied Materials and Interfaces 1, 2829–2834.
Forzani, E.S., Zhang, H.Q., Nagahara, L.A., Amlani, I., Tsui, R., Tao, N.J., 2004. Nano Letters 4, 1785–1788.
Ghica, M.E., Brett, C.M.A., 2005. Analytical Letters 38, 907–920.
Huang, M.H., Mao, S., Feick, H., Yan, H.Q., Wu, Y.Y., Kind, H., Weber, E., Russo, R., Yang, P.D., 2001. Science 292, 1897–1899.
Huang, F.Y., Zhong, Y.M., Chen, J., Li, S.X., Li, Y.C., Wang, F., Feng, S.Q., 2013. Analytical Methods 5, 3050–3055.
Ju, H.X., Leech, D., 1999. Physical Chemistry Chemical Physics 1, 1549–1554.
Jung, J., Lim, S., 2012. Applied Surface Science 265, 24–29.
Kim, S.W., Fujita, S., 2002. Applied Physics Letters 81, 5036–5038.
Li, Y.Y., Zhou, S.Q., 2013. Chemical Communications 49, 5553–5555.
Lee, H.J., Yoon, S.W., Kim, E.J., Park, J.H., 2007. Nano Letters 7, 778–784.
Liu, Z.H., Cho, B., Ouyang, T.M., Feldman, B., 2012. Analytical Chemistry 84, 3403–3409.
Liu, Y., Deng, C.M., Tang, L., Qin, A.J., Hu, R.R., Sun, J.Z., Tang, B.Z., 2011. Journal of the American Chemical Society 133, 660–663.
Liu, J.P., Guo, C.X., Li, C.M., Li, Y.Y., Chi, Q.B., Huang, X.T., Liao, L., Yu, T., 2009. Electrochemistry Communications 11, 202–205.
Lei, Y., Yan, X.Q., Luo, N., Song, Y., Zhang, Y., 2010. Colloids and Surfaces A: Physicochemical and Engineering Aspects 361, 169–173.
Meredith, M.T., Minteer, S.D., 2011. Analytical Chemistry 83, 5436–5441.
Patela, H., Lib, X., Karan, H.I., 2003. Biosensors and Bioelectronics 18, 1073–1076.
Peng, Y., Wei, C.W., Liu, Y.N., Li, J., 2011. Analyst 136, 4003–4007.
Qiu, R., Zhang, X.L., Li, Y., Kim, Y.I., Kang, Y.S., 2007. Chemistry of Materials 19, 4174–4180.
Rahman, M.M., Umar, A., Sawada, K., 2009a. Sensors and Actuators B 137, 327–333.
Rahman, M.M., Oh, K.J., Jeon, I.C., 2009b. Journal of Scientific Research 1, 292–299.
Saha, S., Gupta, V., Sreenivas, K., Tan, H.H., Jagadish, C., 2010. Applied Physics Letters 97, 133704–133713.
Salimi, A., Karimi, R.Z., Noorbakhash, A., Soltanian, S., 2010. Electroanalysis 22, 2434–2442.
Umar, A., Rahman, M.M., Kim, S.H., Hahn, Y.B., 2007. Chemical Communications 2, 166–168.
Umar, A., Rahman, M.M., Hahn, Y.B., 2009a. Electrochemistry Communications 11, 1353–1357.
Umar, A., Rahman, M.M., Hajry, A.A., Hahn, Y.B., 2009b. Electrochemistry Communications 11, 278–281.
Wei, Y.Y., Li, Y., Liu, X.Q., Xian, Y.Z., Shi, G.Y., Jin, L.T., 2010. Biosensors and Bioelectronics 26, 275–278.
Wang, J.P., Thomas, D.F., Chen, A.C., 2008. Analytical Chemistry 80, 997–1004.
Zhao, Y.X., He, Z.Y., Yan, Z.F., 2013a. Analyst 138, 559–568.
Zhao, M.G., Huang, J.Y., Zhou, Y., Chen, Q., Pan, X.H., He, H.P., Ye, Z.Z., 2013b. Biosensors and Bioelectronics 26, 226–230.
Zhao, Z.W., Chen, X.J., Tay, B.K., Chen, J.S., Han, Z.J., Khor, K.A., 2007. Biosensors and Bioelectronics 23, 135–139.
Zang, J.F., Li, C.M., Cui, X.Q., Wang, J.X., Sun, X.W., Dong, H., Sun, C.Q., 2007. Electroanalysis 19, 1008–1014.